

# Lignin in Jute Fabric–Polypropylene Composites

B. A. Acha,<sup>1</sup> N. E. Marcovich,<sup>1</sup> M. M. Reboredo<sup>2</sup>

<sup>1</sup>Chemical Engineering Department, Institute of Materials Science and Technology (INTEMA), University of Mar del Plata, National Research Council (CONICET), B7608FDQ Mar del Plata, Argentina

<sup>2</sup>Materials Engineering Department, Institute of Materials Science and Technology (INTEMA), University of Mar del Plata, National Research Council (CONICET), B7608FDQ Mar del Plata, Argentina

Received 23 July 2008; accepted 2 January 2009

DOI 10.1002/app.29999

Published online 14 April 2009 in Wiley InterScience (www.interscience.wiley.com).

**ABSTRACT:** In this work, the feasibility of using lignin as a compatibilizer for composites made from jute fiber fabric and polypropylene (PP) was studied. Since lignin contains polar (hydroxyl) groups and nonpolar hydrocarbon, it was expected to be able to improve the compatibility between the two components of the composite. It was found that lignin acted as  $\beta$  nucleation, fire retardant, and toughening agent for PP matrix. Jute composites exhibit higher stiffness, tensile strength, and impact behavior in

respect to those of neat PP. Although scanning electron micrographic observations indicate that PP-jute adhesion was slightly improved by lignin addition, additional benefits were only obtained from impact behavior. © 2009 Wiley Periodicals, Inc. *J Appl Polym Sci* 113: 1480–1487, 2009

**Key words:** natural fibers; composites; mechanical properties; thermal properties; lignin; jute

## INTRODUCTION

The use of natural fibers as reinforcement in polymeric matrices has attained great academic and commercial interest in the past decade due to low cost, large availability, and biodegradability of the fibers.<sup>1</sup> Although natural fibers have been used as fillers for thermosetting polymers for some time, cellulosic fillers are being increasingly used nowadays to reinforce thermoplastics. New applications are anticipated. In this sense, thermoplastic composites have received increased attention, particularly for price-driven and high-volume applications.<sup>2</sup> Compatibility between lignocellulosic fiber and polymer plays an important role and severely affects properties of the composite. The interfacial bond strength between lignocellulosic reinforcements and a nonpolar polymer matrix is expected to be poor, due to the hydrophilic nature of the fibers and the hydrophobic thermoplastics. Thus, to obtain a composite with competitive final properties, it is necessary to achieve a good interphase between filler and matrix, generally by the modification of the filler surface or by the addition of compatibilizing agents.<sup>3</sup> However, most filler surface treatments would also increase the cost of these composites (even considering the same processing technique), reducing one of the

incentives to use natural fibers in composites. The use of commercial maleic anhydride grafted polypropylenes (PPMAN) as compatibilizers<sup>4–6</sup> allows the improvement of properties. Some attempts to utilize lignin as a compatibilizer in various polymeric systems have been documented.<sup>2,7–10</sup>

Natural wood and plant fibers are constituted of cellulose fibers, which consist of helical wound cellulose microfibrils, bound together by an amorphous lignin matrix. Lignin acts as a sealant to keep water in the fibers, as a protection against biological attack, and as a stiffener to give the stem its resistance against wind and gravity forces. Besides, lignin is one of the three most abundant renewable resources on the planet, and it is mostly obtained as a waste product during the paper pulping process.<sup>11</sup> Hemicellulose is also found in these natural fibers and is generally believed to be a compatibilizer between cellulose and lignin.<sup>12</sup> Lignins are amorphous and complex phenolic polymers, with rather limited industrial use. They are usually seen as waste products of the pulp and paper industry and are often used as fuel for energy balance for the pulping process.<sup>7</sup> Since lignin contains<sup>13</sup> polar (hydroxyl) groups and nonpolar hydrocarbon and benzene rings, it is expected to be able to improve the adhesion between the two components of the composite, acting as a compatibilizer between hydrophilic natural fiber reinforcement and hydrophobic matrix polymer.<sup>2,12</sup> As lignin is a natural polymer found in wood, it is readily available and relatively inexpensive, although its structure is more or less dependent

Correspondence to: M. M. Reboredo (mrebored@fi.mdp.edu.ar).

on wood species and processing conditions.<sup>14</sup> Besides, lignin is utilized commercially as a stabilizer (antioxidant)<sup>7</sup> for plastics and rubber as well as in the formulation of dispersants, adhesives, and surfactants.<sup>9,14</sup>

The objective of this work was to study the feasibility of using lignin as a compatibilizer in composites made from jute fiber fabric and polypropylene (PP).

## MATERIALS

Commercial bi-directional jute fabric (J) was used as a reinforcement for isotactic PP matrix (Petroquímica Cuyo (Buenos Aires, Argentina), melt index: 11 g/min at 230°C). Properties of jute fiber are: density ( $\rho$ ),  $1.337 \pm 0.05$  g/cm<sup>3</sup>; tensile modulus ( $E$ ),  $19.3 \pm 4.6$  GPa; and tensile strength ( $\sigma_u$ ),  $407 \pm 149$  MPa.<sup>15</sup>

Lignin, in powder form (L, a commercial Kraft lignin: Curan 2711 P) was kindly supplied by Lignotech Sweden. The percentage of lignin was selected according to other compatibilizers usually used for this kind of systems<sup>16</sup>; thus a mixture of PP and 5% lignin (PPL) powder was blended in a heated intensive mixer at 180°C for 10 min.

Films were obtained by compression molding from neat PP and PP/lignin blends at 180°C for 20 min. Each layer of jute fabric was then sandwiched between the films and compression molded at 180°C for 25 min. The jute fabric was dried in a vacuum oven at 70°C before the preparation of the composites. The reinforcement average content of the composites was 25 wt %.

## EXPERIMENTAL

Thermogravimetric tests were performed using a Seiko Instruments SII Exstar 6000 thermogravimetric analyzer (TGA, Chiba, Japan). The measurements were carried out in air atmosphere from room temperature to 600°C at a heating rate of 10°C/min. The curves are reported as percent weight loss as a function of temperature. Sample weight was about 5 mg.

Thermal behavior of the PP and PPL blend was analyzed by differential scanning calorimetry (DSC) using a Perkin-Elmer Pyris 1 (Norwalk, CT) instrument equipped with an intercooler 11 as cooling unit, operating under a nitrogen atmosphere (20 mL/min). The measurements were performed according to the following cycle: heating from 25 to 200°C at 10°C/min (to erase any previous morphological history), cooling down to room temperature at different cooling rates (1, 10, and 60°C/min) to study the crystallization process, and finally heating from 25 to 200°C at 10°C/min again to observe the melting behavior.

The qualitative analysis of crystalline phases present in the polymer was carried out by X-ray diffraction

(XRD) using a Philips equipment PW 1830 (Eindhoven, The Netherlands) (Co K $\alpha$  radiation; Ni-filtered at 40 kV and 30 mA; wavelength = 0.172 nm).

Dynamic mechanical properties were measured in a Dynamical Mechanical Thermal Analyzer (EPLEXOR 150N, Gabo Qualimeter, Ahlden, Germany). The tests were carried out using a frequency of 10 Hz and a heating rate of 1°C/min, from -100 to 150°C. Tensile fixture was used. The size of the specimens was 50 mm  $\times$  10 mm  $\times$  3 mm, where the linear dimensions were measured up to 0.01 mm.

Tensile tests were performed according to the ASTM D 638 standard, using an Instron 8501 universal testing machine (Buckinghamshire, England) at a crosshead speed of 5 mm/min. Young (tensile) modulus ( $E$ ), tensile strength ( $\sigma_u$ ), and strain at break ( $\epsilon_u$ ) were determined from the stress-strain curves. At least five samples were tested in all cases.

Instrumented falling weight impact (IFWI) tests were carried out at room temperature using a CEAST Fractovis (Torino, Italy) drop tower at room temperature using the molded plaques, with a striker speed of 1 m/s and a mass of 18.5 kg. The thickness-related perforation energy was computed from the IFWI test fractograms. At least four tests were performed in all cases. From the IFWI fractograms the following parameters were determined<sup>15,17</sup>:

The maximum strength ( $\sigma_{\max}$ ), which represents the impact bending strength at crack initiation, was:

$$\sigma_{\max} = \frac{2.5F_{\max}}{t^2} \quad (1)$$

where  $F_{\max}$  is the maximum load registered in the fractogram and  $t$  is the sample thickness.

The energy at crack initiation ( $E_i$ ) normalized by thickness was:

$$E_i = \frac{1}{t} \int_0^{X_{\max}} FdX \quad (2)$$

where  $X_{\max}$  is the displacement at maximum load.

The total energy required for penetrating the specimen completely ( $E_t$ ), normalized by thickness was:

$$E_t = \frac{1}{t} \int_0^{X_{\text{total}}} FdX \quad (3)$$

where  $X_{\text{total}}$  is the total displacement (until the end of the test).

The propagation energy, which is the energy required to complete disk penetration ( $E_p$ ), was:

$$E_p = E_t - E_i \quad (4)$$

Scanning electron micrographs from tensile fracture surfaces were taken with a scanning electron

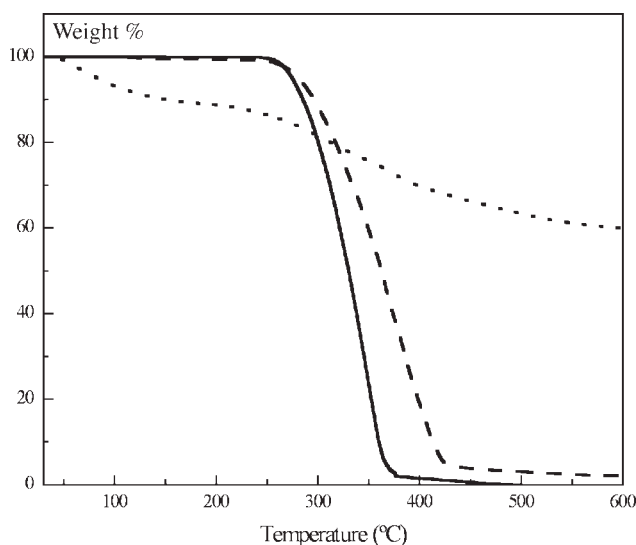


**Figure 1** Thermogravimetric curves of mass loss versus temperature for PP, L, and PPL blend. Pure PP (solid line), L (dotted line), PPL 95/5 (dashed line).

microscope (SEM) Philips model SEM 505 (Eindhoven, The Netherlands). The samples were previously coated with gold.

## RESULTS AND DISCUSSION

### Characterization of Polypropylene–Lignin Blends

Figure 1 shows the thermal degradation patterns in air atmosphere for L, PP, and PPL blend registered at 10°C/min. The beginning of thermal degradation ( $T_i$ ) was taken at 5% of the weight loss after 100°C to ensure elimination of absorbed moisture. This temperature for L is around 226°C. Its aromatic chemical structure is able to give a very high char yield (around 60% at 600°C). It is well known that the ability to form char during the thermal degradation is a basic aspect of flame retardant additives, since the char reduces the combustion rate of polymeric materials because it does not allow the oxygen to reach the combustion zone easily.<sup>18</sup>

On the other hand, thermal degradation of neat PP takes place in one step, which begins at 272°C and finishes at about 450°C without char formation. The curve for the PPL (95/5) blend shows a higher degradation initial temperature, compared with pure PP, and presents little char yield. These results ( $T_i$ ) are summarized in Table I, together with the temperature at which half the amount of the initial mass of the material is lost ( $T_h$ ) and char percentage produced at 600°C, for PP, L, and several PPL blends. It is noticed that the incorporation of 5 wt % of lignin increases the thermal degradation temperature of the pure PP at about 8°C and the char yield at about 2 wt %. However, the main change is in  $T_h$ , an increase of almost 35°C in comparison with that of

the neat PP is obtained. It can be explained by the fact that although lignin begins to degrade several degrees before PP, when PP degradation starts, its hydrocarbon radicals are formed in the presence of charring lignin and the interactions between them allow shield formation, leading to a reduced combustion rate. A synergetic effect is observed for the initial thermal degradation temperature when lignin is blended with PP, since the resulting effect of two components taken together is greater ( $T_{iPPL} = 280^\circ\text{C}$ ) than their individual effect ( $T_{iPP} = 272^\circ\text{C} - T_{iL} = 226^\circ\text{C}$ ).<sup>19</sup> On the other hand, lignin never loses half the amount of the initial mass. Nevertheless, as the lignin content increases,  $T_i$  decreases, due to the lower degradation temperature of lignin, but a large increase in char yield is noticed. Further increments in lignin (beyond 15%) do not produce any improvements in the thermal stability of polypropylene blends, as was also observed by other researchers.<sup>20</sup>

Figure 2 shows the thermograms of the second heating step for PP and PPL (95/5) samples after different cooling rates. It is observed that a symmetric endothermic peak occurs between 163 and 167°C for both PP and PPL samples if the cooling rate is lower than 10°C/min. These peaks correspond to the melting of the  $\alpha$ -crystalline phase of the PP and exhibit a maximum at  $T_m = 163^\circ\text{C}$  for PP and 167°C for PPL blend. The addition of lignin produces a shift of the melting peak to higher temperatures. Normally, there is one fusion peak for a given crystalline phase in DSC tests, although the temperature range for the melting process and the melting temperature may vary, depending on the degree of perfection of the crystals. A higher melting point and a narrower temperature range are expected for the fusion of more perfect crystals, as was stated in relevant literature.<sup>21–24</sup>

The peaks for both systems become less symmetric as the cooling rate increases until 60°C/min, and additional peaks appear (around 160°C for PP and about 155°C for PPL blend). These peaks are attributed to the recrystallization (or reorganization) of the imperfect crystals formed during the cooling step since they did not have enough time to perfect themselves and would undergo perfection during

**TABLE I**  
Thermal Degradation Parameters of PPL Blends

PPL	$T_i$ (°C)	$T_h$ (°C)	Char yield (wt %) <sup>a</sup>
100/0	272	331	0
95/5	280	365	2.1
90/10	256	335	3.2
85/15	250	355	13.1
80/20	251	343	11
0/100	226	–	59.7

<sup>a</sup> At 600°C.

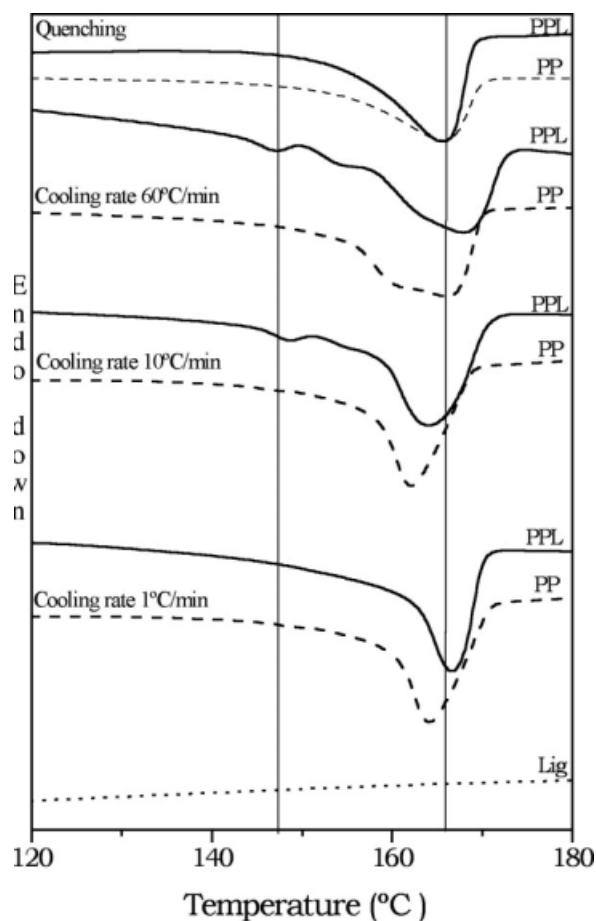


**Figure 2** DSC second heating scanning curves after cooling crystallization at different cooling rates of pure PP and PPL blend. Heating rate: 10°C/min.

heating. Moreover, a new endothermic peak appeared for the PPL blend at lower temperatures (approximately at 148°C) for intermediate cooling rates (from 10 to 60°C/min). It is attributed to the melting of the  $\beta$ -crystalline form of PP. Thus, lignin acts as a  $\beta$  nucleation agent for the PP matrix, although the amount of  $\beta$ -crystalline phase formed is rather low, as observed from the small peaks detected.

It was also found that the area of the  $\beta$ -peak increases as the cooling rate increases, but at very high cooling rates (quenched samples were obtained by immersing them in cold water) the  $\beta$ -phase formation is suppressed, as observed in the corresponding thermogram. The formation of this new crystalline phase was further studied by X-ray measurements.

The  $\alpha$ -PP form is the most common and stable. However, in many applications of PP, the  $\beta$  form can be present in considerable amounts. In samples that have been subjected to high orientation or deformation in the molten state, the  $\beta$  form can be found. Injection-molded and extruded PP samples usually show a skin-core morphology (the  $\beta$  structure is located at the skin of these samples). More-

over, the  $\beta$  form can also be promoted with respect to the  $\alpha$  form by specific crystallization conditions: high cooling rates, high crystallization temperatures or large temperature gradients.<sup>19,21,24,25</sup> Besides, the  $\beta$  phase can be obtained by crystallization in the presence of special nucleation agents, i.e., dye quinaclidone<sup>18</sup> and pimelic acid/calcium stearate.<sup>25,26</sup>

The diffractograms shown in Figure 3 were taken from PPL samples cooled from the melt temperature by convection to stagnant, room temperature air or by quenching in cold water. Both diffractograms show the  $\alpha$  phase characteristic peaks at scattering angles of 16.3°, 19.7°, 21.9°, and 24.7°. Nevertheless the samples cooled in stagnant air exhibit the  $\beta$ -phase peaks (at  $2\theta = 18.6^\circ$  and  $24.6^\circ$ , respectively)<sup>19,26</sup> but they are absent when quenching was applied. This suggests that the  $\beta$ -phase production can be influenced by the thermal conditions<sup>18</sup> during the PP crystallization in the presence of an appropriate nucleating agent.

The order of perfection of the PP crystals is strongly related to the crystal size,<sup>22</sup> thus, from the diffractograms of Figure 3, the crystal size of the  $\alpha$  phase was calculated using the Scherrer equation, with  $K = 0.9$ .<sup>29</sup> For the determination, the most intense crystalline reflection (110) of the  $\alpha$  crystals, corresponding to the crystal growing planes and, consequently, to the largest lateral dimensions of lamellar crystallites, was selected. The  $\alpha$  crystal size of the PPL samples quenched was 13.75 nm, whereas in the samples cooled by convection it was 16.62 nm. Thus, from comparison between Figures 2 and 3, it can be concluded that a higher melting temperature and a sharp melting peak are consistent with

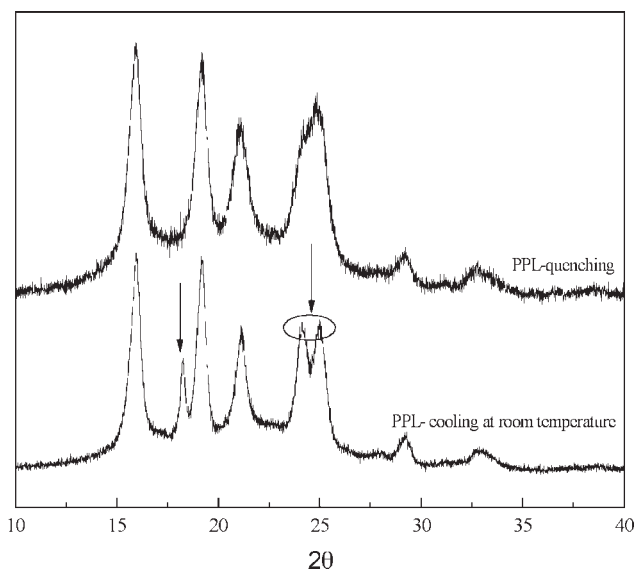


**Figure 3** X-ray diffraction spectra of PPL sample cooled from the melt temperature by (a) convection to stagnant air and (b) by quenching in cold water.



**TABLE II**  
Tensile Properties of PP, PPL, and Composites

	Modulus (GPa)	$\varepsilon_u$ (mm/mm)	$\sigma_u$ (MPa)
PP	0.9 ± 0.1	0.15 ± 0.03	27.2 ± 0.8
PPL	1.0 ± 0.1	0.077 ± 0.002	23.9 ± 0.3
PPJ	2.4 ± 0.1	0.030 ± 0.003	39.7 ± 5.8
PPLJ	2.3 ± 0.2	0.026 ± 0.001	36.4 ± 2.7

the large crystal size observed from X-ray, even when  $\beta$  crystalline phase is formed.

### Mechanical Properties of PPL Bends and Composites

Table II shows the tensile properties for pure PP, PPL, jute-PP (PPJ), and jute-PP/L (PPLJ) composites. The incorporation of lignin does not produce any important changes in the modulus because the quantity is small enough to produce a significant modification. Nevertheless, the strength decreases  $\sim 12\%$  in respect to that of the neat PP, and the strain at break decreases  $\sim 50\%$ . This reduction is mainly attributed to the rigidity that the lignin particles impart to the pure matrix, even though the content is low. It is well known that the addition of rigid filler to thermoplastics considerably reduces the tensile strain at break by reducing the amount of material available to deform.<sup>30</sup> On the other hand, the addition of jute fabric increases both the modulus and strength and decreases markedly the strain at break due to the low deformation of the jute fibers, which leads to the cavitation between the fibers and the matrix, contributing to the formation of weak points inside the composite. However, no further improvement occurred due to the addition of lignin, probably because lignin is a network polymer (a rigid molecule unable to form entanglements with PP, as compared with the traditional PPMAN compatibilizers). Besides, there is the possibility that the  $-\text{OH}$  groups present in the lignin may be in a condensed state (since it was used as received), which renders the groups less reactive toward jute fiber (in comparison with traditional PPMAN compatibilizers), as observed by Rozman et al.<sup>2</sup> In this sense, contradictory results were found in literature: Rozman et al.<sup>2</sup> indicated that the addition of lignin as a compatibilizer for coconut fiber-polypropylene composites enhances their flexural behavior (in comparison to those of control composites) but do not improve tensile properties. However, in a previous paper<sup>31</sup> they showed that lignin (added externally) plays a positive role in improving the tensile strength of rubberwood-PP composites. Moreover, Thielemans and Wool<sup>12</sup> showed by SEM that the addition of butyrate kraft lignin improved the interface between an

unsaturated resin and long flax fibers but decreases the mechanical (both flexural and tensile) properties of the overall composite. They demonstrated that this is caused by the increased resin viscosity after lignin addition, which decreased fiber wetting and resin penetration.

Dynamic mechanical properties such as the storage modulus ( $E'$ ) and  $\tan \delta$  of PP, PPL, and their composites (PPJ, PPLJ) were studied as a function of temperature. Figure 4(a) shows that the storage modulus of the materials decreased as temperature increased. With a rise in temperature, the advantages of the fiber reinforcement increase significantly, since the increasing mobility of the polymer macromolecules is counteracted by the rigidity of the fibers. The storage modulus of jute composites was improved in about 35% in the glassy zone ( $\approx -50^\circ\text{C}$ ) and in about 290% in the rubbery region ( $\approx 80^\circ\text{C}$ ), compared with both matrices. It was also found that the storage moduli of the lignin containing systems (PPL, PPLJ) were slightly higher than those of the materials without it (PP, PPJ).

The loss modulus ( $E''$ ) peaks of composites were shifted toward lower temperatures compared with both PP and PPL [Fig. 4(b)]. This minor decrease in glass transition temperature ( $T_g$ ) is attributed to the small quantities of water that could be retained by the jute fibers. The ratio of storage and loss modulus ( $\tan \delta = E''/E'$ ) is shown in Figure 4(c). The area under the  $\tan \delta$  curve becomes smaller for composites with respect to that of the neat PP, since the polymer content is decreased to the same extent and only the amorphous phase of the partially crystalline PP is involved in the glass transition. Moreover, the area of  $\tan \delta$  peak is slightly lower for PPL than for neat PP because chain movements are also restricted by the presence of lignin particles. Regarding the width of PPL  $\tan \delta$  peak, it also becomes broader than that of the neat matrix ( $25.83^\circ\text{C}$  and  $24.17^\circ\text{C}$ , respectively). Particulate fillers, even when present in low concentrations, as in this case, increase the damping by the introduction of new mechanisms that are not present in the pure polymer, i.e., particle-particle friction, where particles touch one another as in weak agglomerates, particle-polymer friction, where there is essentially no adhesion at the interface, and excess damping in polymer near the interface because of the induced thermal stresses or changing in polymer conformation or morphology.<sup>32</sup>

The impact performance of composites was evaluated and compared with that of the neat PP. Table III shows the results for all the materials. The initiation energy ( $E_i$ ) is lower for the composites than for the neat PP and the PPL blend, indicating that the crack begins at smaller loads and sooner during the test because some fibers are probably acting as initiation points of fracture. Nevertheless, the total

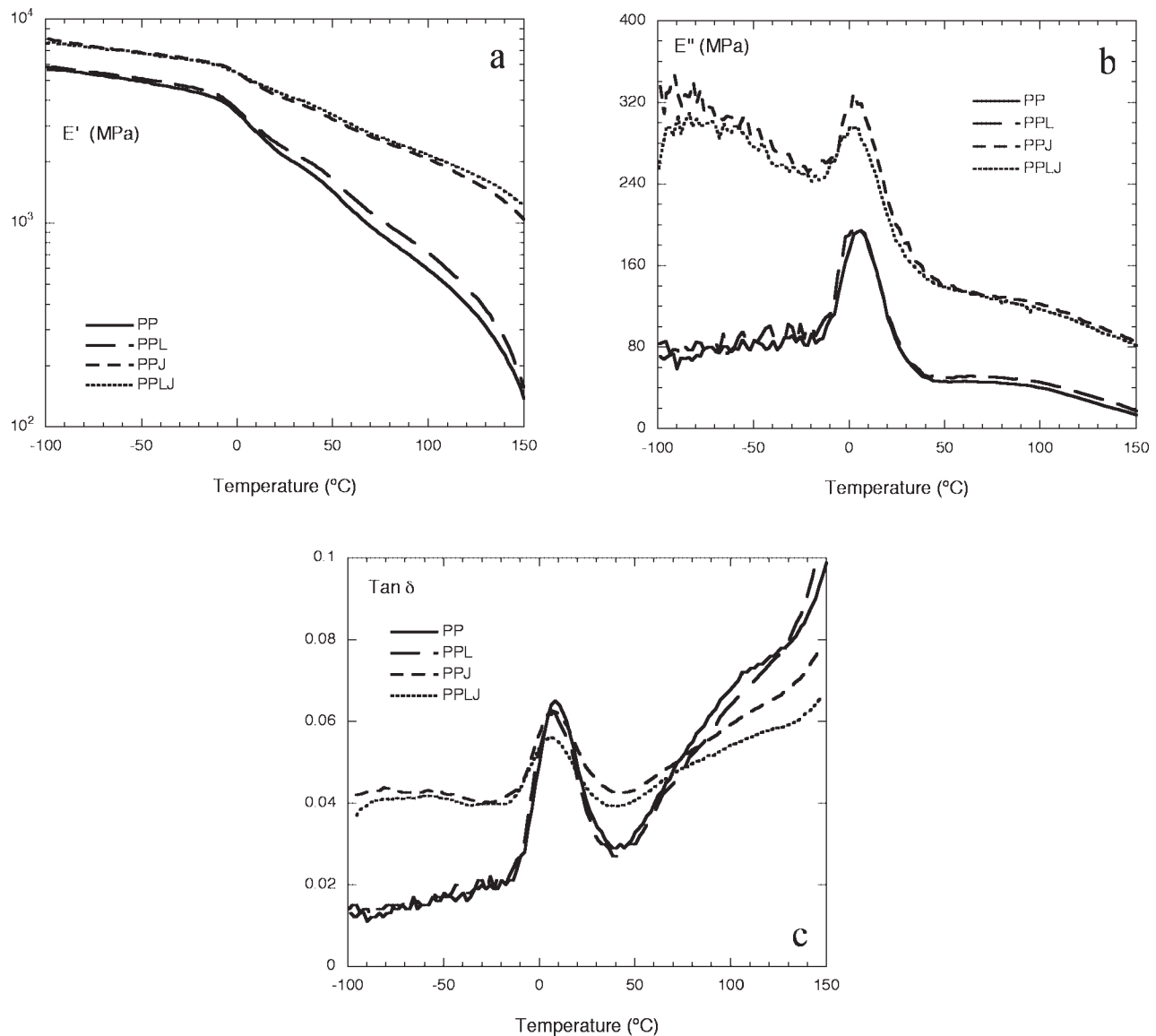


**Figure 4** Temperature scans of (a) storage modulus,  $E'$ ; (b) loss modulus,  $E''$  and (c)  $\tan \delta$  of neat PP, PPL, and its jute-reinforced composites.

energy ( $E_i$ ) absorbed during the impact test considerably increases for the composites with respect to that of the neat PP, because the fibers introduce other well-known mechanisms of energy consumption (fiber deformation, debonding, fiber failure, and pull-out) that do not exist in the pure matrix. The propagation energy is similar for both composites. Nevertheless, lignin has a clear effect on the energy

at crack initiation, as  $E_i$  of PPLJ is 38% higher than  $E_i$  of PPJ.

It is interesting to notice the important increase in the total absorbed energy when lignin alone is added at levels as low as 5% (PPL system). The energy is about the same of composite materials and much higher than pure PP. Lignin acts as a toughening agent, increasing the propagation energy ( $E_p$ ),

**TABLE III**  
Impact Properties of PP, PPL, and Composites

	Modulus (GPa)	$E_i$ (J/mm)	$E_i$ (J/mm)	$E_p$ (J/mm)	$\sigma_{\max}$
PP	$1.20 \pm 0.08$	$0.17 \pm 0.02$	$0.17 \pm 0.02$	0	$39.2 \pm 2.3$
PPL	$1.18 \pm 0.12$	$0.188 \pm 0.106$	$1.01 \pm 0.06$	$0.82 \pm 0.05$	$23.9 \pm 0.3$
PPJ	$2.49 \pm 0.35$	$0.098 \pm 0.012$	$1.09 \pm 0.06$	$0.99 \pm 0.08$	$62.5 \pm 7.6$
PPLJ	$1.85 \pm 0.12$	$0.135 \pm 0.003$	$1.10 \pm 0.03$	$0.96 \pm 0.03$	$59.1 \pm 3.2$

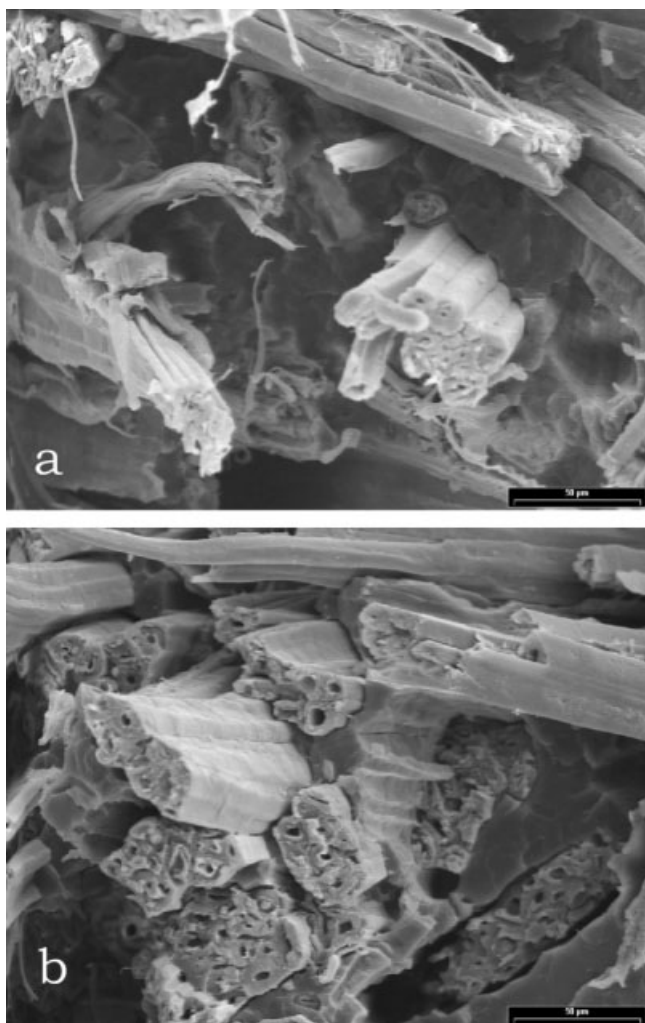


**Figure 5** Scanning electron micrographs taken from the fracture surface of the tensile specimens: (a) PPJ, and (b) PPLJ.

and thus improving the PP impact behavior. Some controversy still exists regarding the precise mechanisms responsible for the observed improvements in toughness in brittle polymers reinforced with rigid fillers. Several authors have suggested that the presence of the rigid particles serves to pin the advancing crack, forcing it to bow out and hence increasing the fracture energy.<sup>33–35</sup> Moreover, Kim and Michler<sup>36</sup> stated that when dealing with rigid particle filled-PP (this case), the filler cannot be deformed by external stress in the specimen but acts only as stress concentrators during the deformation processes. Additionally, they stated that when the filler particles form agglomerates, and although the agglomerates consist of numerous small rigid filler particles, they act on the whole, similar to rubber modifier particles during the deformation processes.

A clear increase in the impact strength and modulus in respect to that of the pure PP was found for both composites. The addition of fibers to the poly-

propylene increases the stiffness, thus raising the disk modulus, but again the addition of lignin to the composite does not improve the impact behavior.

### Microscopy

Figure 5 shows the fracture surface of composites. Fiber pull-out is observed in both cases (PPJ and PPLJ), but the pulled fiber length of the pulled fibers is slightly shorter in the PPLJ [Fig. 5(b)] than in the PPJ [Fig. 5(a)] composites.

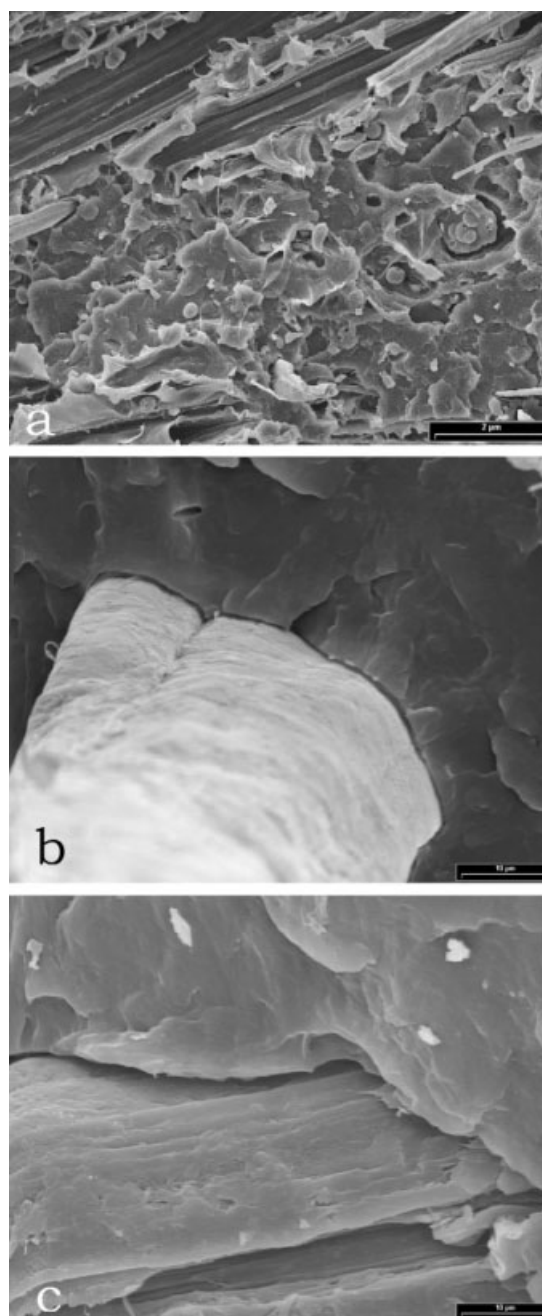


**Figure 6** Scanning electron microscopy micrographs taken from the fracture surface of tensile specimens: (a) PPL, (b) PPLJ, and (c) PPJ.

Micrographs with higher magnification for PPL [Fig. 6(a)] and PPLJ [Fig. 6(b)] show that the PPL blend as well the matrix around of the jute fiber are homogeneous. This fact is a clear indication of good distribution of the lignin particles into the polypropylene matrix but also means that during composite processing, lignin particles did not migrate to the fiber-matrix interface.

Moreover, Figure 6(b,c) shows that the fiber-matrix separation is smaller for the PPLJ than for the PPJ, which means that the adhesion between fiber and matrix is slightly increased in respect to that of the PPJ sample. Nevertheless, and according to the previous results, this improvement is not enough to improve the mechanical behavior in general. Analyzing these micrographs and the mechanical results as a whole, it is possible to conclude that in this case lignin is acting more as a filler than as a coupling agent.

## CONCLUSIONS

TGA results confirmed the role of lignin as a fire retardant when mixed in polypropylene, even though the amounts used in this work were low when compared with the usual amounts of fire retardant agents used in PP.

It was confirmed by DSC and X-ray analysis that PP crystallized simultaneously into two crystalline forms,  $\alpha$  and  $\beta$ , in the presence of lignin. An increase of  $\beta$ -form fraction was observed with the increase of cooling rate (for intermediate cooling rates).

The addition of jute fabric to PP leads to a significant increase in the stiffness of the composite due to the higher modulus of the jute fibers. Jute fabric also improved the tensile strength and the impact behavior in respect to those of neat PP. The addition of only lignin to the PP increased the impact energy and decreased the strain at break. However, and although SEM observations indicate that PP-jute adhesion was slightly improved by lignin addition, the mechanical behavior of the composites was not improved in general.

The authors thank the National Research Council of Argentina (CONICET), the National University of Mar del Plata (UNMDP), and the Institut für Verbundwerkstoffe GmbH (IVW), Kaiserslautern (Germany).

## References

- Brouwer, W. D. *SAMPE J* 2000, 36, 18.
- Rozman, H. D.; Tan, K. W.; Kumar, R. N.; Abubakar, A.; Mohd Ishak, Z. A.; Ismail, H. *Eur Polym J* 2000, 36, 1483.
- Gauthier, R.; Joly, C.; Coupas, A. C.; Gauthier, H.; Escoubes, M. *Polym Compos* 1998, 19, 287.
- Kazayawoko, M.; Balatincez, J. J.; Matuana, L. M. *J Mater Sci* 1999, 34, 6189.
- Gassan, J.; Bledzki, A. K. *Compos A* 1997, 28, 1001.
- Ichazo, M. N.; Albano, C.; González, J.; Perera, R.; Candal, M. V. P. *Compos Struct* 2001, 54, 207.
- Pouteau, C.; Dole, P.; Cathala, B.; Averous, L.; Boquillon, N. *Polym Degrad Stab* 2003, 81, 9.
- Rozman, H. D.; Tan, K. W.; Kumar, R. N.; Abudakar, A. *Polym Int* 2001, 50, 561.
- Alexy, P.; Košíková, B.; Podstránska, G. *Polymer* 2000, 41, 4901.
- Rozman, H. D.; Tan, K. W.; Kumar, R. N.; Abudakar, A. *J Appl Polym Sci* 2001, 81, 1333.
- Hatfield, R. D.; Ralph, J. *Should Lignin be Redefined? Research Summaries*; U.S. Dairy Forage Research Center, Madison, Wisconsin, 1997; pp 31-34.
- Thielemans, W.; Wool, R. P. *Compos A* 2004, 35, 327.
- Feldman, D.; Banu, D.; Campanelli, J.; Zhu, H. *J Appl Polym Sci* 2001, 81, 861.
- Kadla, J. F.; Kubo, S. *Compos A* 2004, 35, 395.
- Acha, B. A.; Reboredo, M. M.; Marcovich, N. E. *Polym Int* 2006, 55, 1104.
- Karnani, R.; Krishnan, M.; Narayan, R. *Polym Eng Sci* 1997, 37, 476.
- Mouzakis, D. E.; Harmia, T.; Karger-Kocsis, J. *Polym Polym Comp* 2000, 8, 167.
- De Chirico, A.; Armanini, M.; Chini, P.; Cioccolo, G.; Provasoli, F.; Audisio, G. *Polym Degrad Stab* 2003, 79, 139.
- Canetti, M.; De Chirico, A.; Audisio, G. *J Appl Polym Sci* 2004, 91, 1435.
- Gregorová, A.; Cibulková, Z.; Kosíková, B.; Simon, P. *Polym Degrad Stab* 2005, 89, 553.
- Li, J. X.; Cheung, W. L. *J Mater Process Technol* 1997, 63, 472.
- Ferrer-Balas, D.; MasPOCH, M. L.; Martinez, A. B.; Santana, O. O. *Polymer* 2001, 42, 1697.
- Shangguan, Y.; Song, Y.; Peng, M.; Li, B.; Zheng, Q. *Eur Polym J* 2005, 41, 1766.
- Varga, J. In *Polypropylene Structure, Blends and Composites*; Karger-Kocsis, J., Ed.; Chapman and Hall: London, 1995; Vol. 1.
- Núñez, A. J.; Kenny, J. M.; Reboredo, M. M.; Aranguren, M. I.; Marcovich, N. E. *Polym Eng Sci* 2002, 42, 733.
- Vleeshouwers, S. *Polymer* 1997, 38, 3213.
- Saujanya, C.; Radhakrishnan, S. *Polymer* 2001, 42, 6723.
- Obadal, M.; Cermák, R.; Raab, M.; Verney, V.; Commereuc, S.; Fraïsse, F. *Polym Degrad Stab* 2005, 88, 532.
- Klug, H. P.; Alexander, L. E. *X-ray Diffraction Procedures for Polycrystalline and Amorphous Materials*; Wiley: New York, 1974; pp 618-708.
- Richardson, M. O. W. *Polymer Engineering Composites*; Applied Science Publishers: London, 1977; Chapter 2.
- Rozman, D.; Kumar, R. N.; Addli, M. R. M.; Abusamah, A.; Mohd Ishak, Z. A. *J Wood Chem Tech* 1998, 18, 471.
- Pothan, L. A.; Oommen, Z.; Thomas, S. *Compos Sci Technol* 2003, 63, 283.
- Spanoudakis, J.; Young, R. J. *J Mater Sci* 1984, 19, 473.
- Moloney, A. C.; Kausch, H. H.; Stieger, H. R. *J Mater Sci* 1983, 18, 208.
- Perek, J.; Pilliar, R. M. *J Mater Sci Med* 1992, 3, 333.
- Kim, G.-M.; Michler, G. H. *Polymer* 1998, 39, 5689.